N87-16032

MAST FLIGHT SYSTEM DYNAMIC PERFORMANCE

L. Davis

D. Hyland

T. Otten

F. Ham

First NASA/DOD CSI Technology Conference
Norfolk, Virginia
November 18-21, 1986

PRECEDING PAGE BLANK NOT FILMED

This discussion focuses on the MAST Flight System as a test bed for large space structure control algorithms. After giving an overview of the whole system, four main topics will be covered: the actuators, the sensors, the control computer, and the baseline damping algorithm.

MAST FLIGHT SYSTEM DYNAMIC PERFORMANCE

1. Overview of the control system architecture
2. Placement of sensors and actuators
3. LDCM design and performance
4. Sensor performance and models
5. Computer architecture and performance
6. Baseline damping system performance

CONTROL SYSTEM ARCHITECTURE

The system to be controlled is the 54-bay mast. Sensors and actuators are placed at the various stations indicated. The control computer system communicates with the sensors and actuators via a 1553 data bus.

The actuators are Harris-designed Linear DC Motors (LDCMs). Ten of these actuators are placed at various stations along the length of the mast. The four larger, Type I actuators are placed at the tip to provide control over both the primary bending modes and the torsion modes. The remaining, Type II actuators provide good control authority over the second and third bending modes.

The control sensors consist of 18 linear accelerometers, 5 angular accelerometers, and 6 rate gyros. Sensors are collocated with the actuators and placed at additional locations to measure the motion of the structure accurately. The signal-to-noise ratio is at least 40 dB for signals to be expected during the experiment.

The control computer system samples all sensors and commands all actuators at a rate of 150 Hz. The control computations are performed in the EDS computer, while the MDIS computer handles communications both with the sensors and actuators and with the Shuttle.

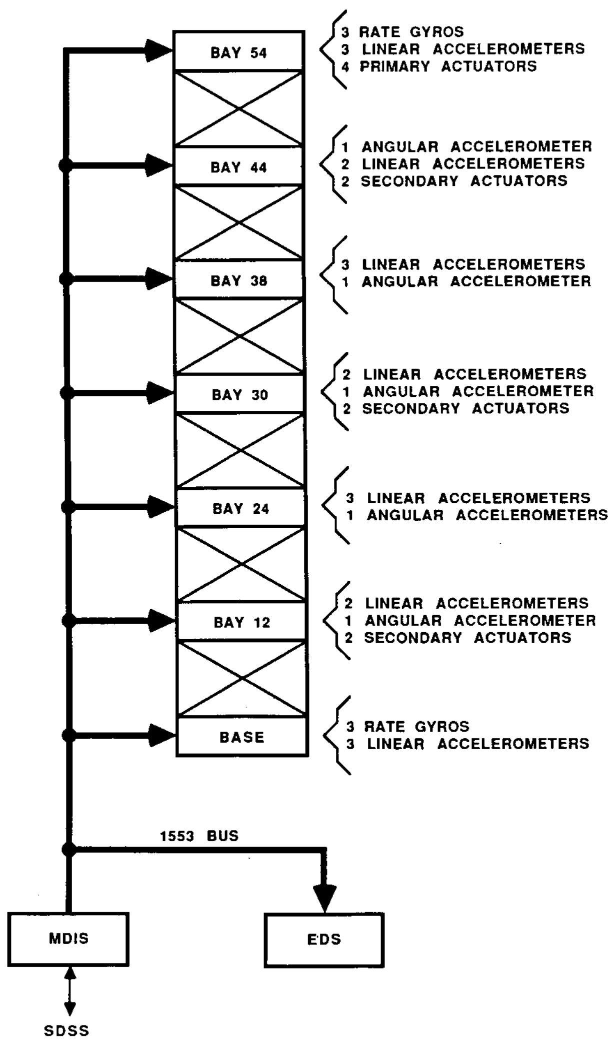

TYPE 1 LDCM

The Linear DC Motors (LDCMs) were designed by Harris to act as the control actuators for the MAST Flight System. Each LDCM consists of two pieces: the fixed primary, which houses the motor coils, and the moving secondary, which houses the permanent magnets and provides the reaction mass for the actuator.

The primary coils are rigidly mounted to the motor frame. They are switched to varying currents based on the commanded force and the position of the moving secondary as measured via the commutation vanes. The fixed coils rest between the return irons and the permanent magnets of the secondary. The eight bearings ensure that the secondary remains centered laterally while keeping friction to a minimum.

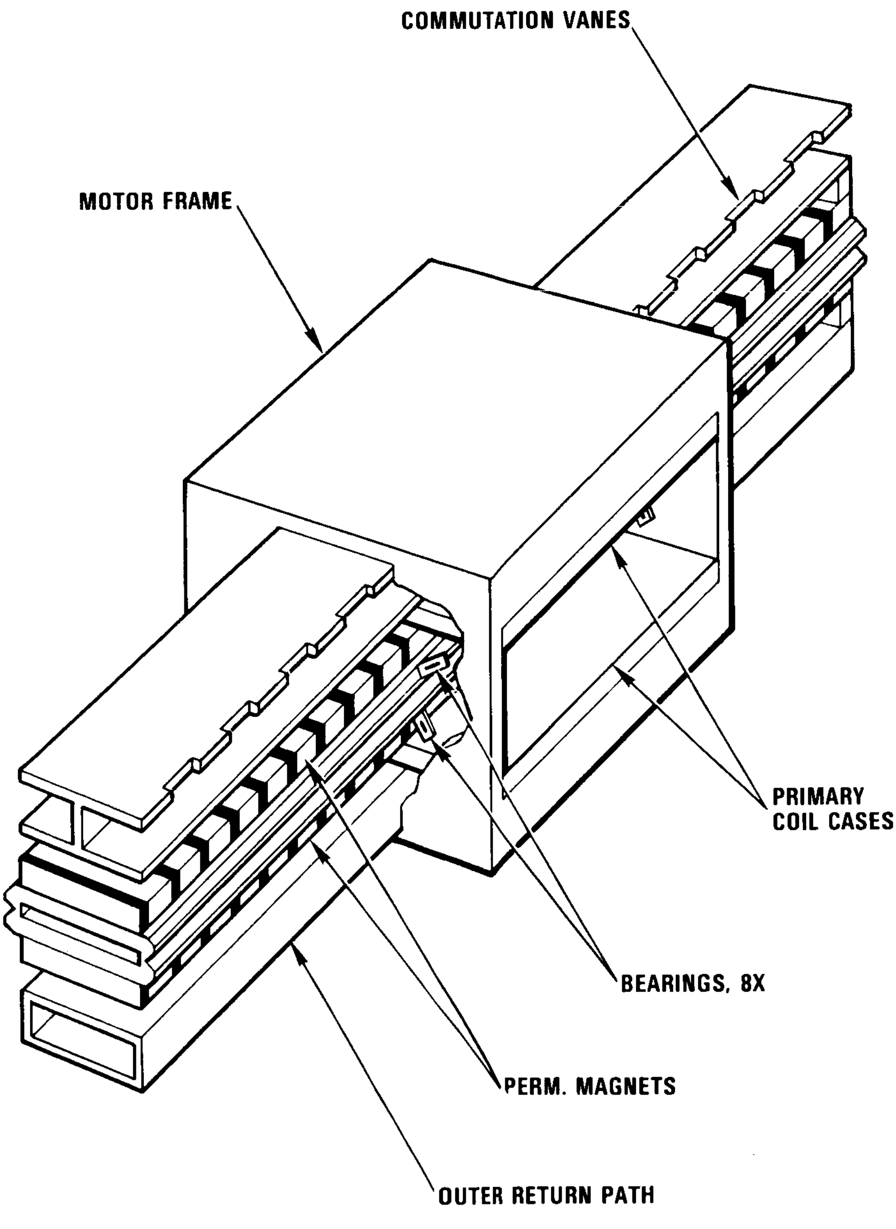

The LDCMs are compensated to provide the user full access to the capabilities of the devices while ensuring that they operate within their limitations of stroke and force.

The compensation works, in the absence of user input, to keep the LDCM secondary fixed in inertial space in spite of transient mast motion. This serves to decouple the operation of the LDCM from the dynamics of the mast. In this mode, the stroke of the actuator must be divided between the motion of the mast and the motion due to control inputs. The total stroke of the device minus the allowed motion of the mast becomes the effective stroke available for control.

The transfer function as seen by the user through the EDS command is tailored to give access to the full stroke capability at low frequencies and the full force capability at high frequencies. The limit on the user command ensures that the LDCM does not exceed these capabilities.

POSITION LOOP OPERATION

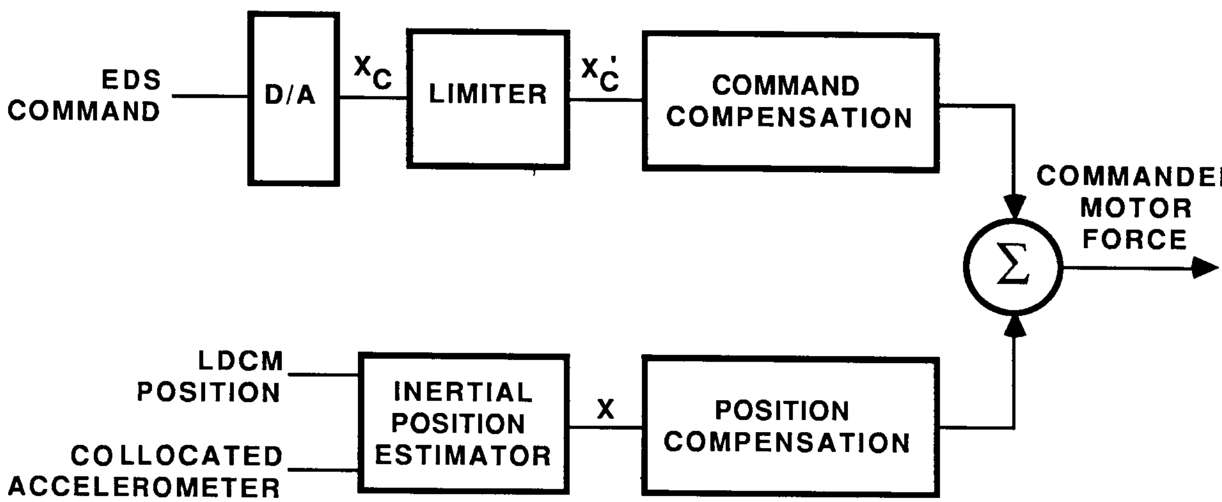

EQUIVALENT USER MODEL

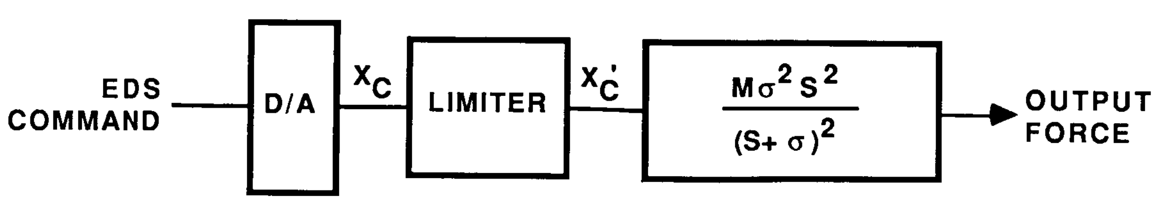

COMPENSATED LDCM SPECIFICATIONS

The overall specifications for the compensated LDCMs are shown below. The mass differential between the Type I and Type II actuators, combined with their allowed stroke limitations, combine to determine the compensated bandwidth sigma. The user command is limited by a single value such that at low frequencies the stroke is not exceeded. The bandwidth is then adjusted such that at high frequencies the force limit is not exceeded.

The user has access to the relative position of the secondary with respect to the primary of each LDCM. This accurate measurement comes from the commutation vanes of the secondary.

Accurate knowledge of relative secondary position has allowed Harris to reduce force ripple below 1% of nominal output force and additive force errors due to position feedback below 0.05 N, thus providing users with a quiet actuator for vibration suppression.

TRANSFER FUNCTION: $\dfrac{\text{FORCE OUT}}{\text{CMD IN}} = \dfrac{m\sigma^2 S^2}{(S+\sigma)^2}$

$m = 11$ Kg, $\sigma = 2\pi$ RAD/SEC (TIP)

$m = 7$ Kg, $\sigma = 5.5$ RAD/SEC (INTERMEDIATE)

STROKE: ±15 cm (TIP)
± 7 cm (INTERMEDIATE)

FORCE OUTPUT: ±30 N (TIP)
±15 N (INTERMEDIATE)

POSITION MEASUREMENT
RESOLUTION: ±0.48 mm

OUTPUT NOISE: RIPPLE <1% OF OUTPUT
0.05 Nt RANDOM ADDITIVE

SENSOR SPECIFICATIONS

The sensor complement has been chosen to measure the expected signals with 40 dB of signal-to-noise ratio. In some cases, the 12 bits of digital information available to the computer were not enough to reflect the accuracy of the sensor. Low ranges are used to expand the dynamic range seen by the computers.

LINEAR ACCELEROMETERS:

RANGE:	+/- 1.0 G (HIGH RANGE) +/- 0.1 G (LOW RANGE)
RESOLUTION:	500 MICRO-G (HIGH RANGE) 50 MICRO-G (LOW RANGE)
BANDWIDTH:	0-50 Hz MIN. (150 Hz MAX.)

ANGULAR ACCELEROMETERS:

RANGE:	+/- 10 RAD/SEC^2
RESOLUTION:	0.01 RAD/SEC^2
BANDWIDTH:	0-40 Hz MIN. (200 Hz MAX.)

ANGULAR RATE GYROS:

RANGE:	+/- 1 DEG/SEC
RESOLUTION:	0.0005 DEG/SEC
BANDWIDTH:	0-80 Hz

STRAIN GAUGES:

RANGE:	+/- 7500 MICROSTRAIN
RESOLUTION:	50 MICROSTRAIN

THERMISTERS:

RANGE:	+/- 100 DEG C.
RESOLUTION:	0.5 DEG C.

SENSOR MODELS

The sensors to be used for control are inertial. They conform roughly to the models shown below. The indicated noises are white, zero-mean processes. Their intensities were chosen to reflect either the resolution of the sensor or the manufacturers' estimates of rms noise amplitude, whichever was coarser. The bandwidths are the lowest available for the type of sensor under consideration.

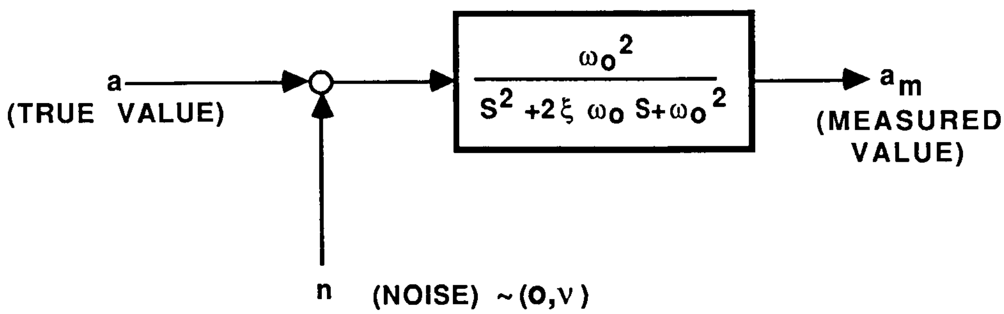

$$\left.\begin{aligned} \omega_o &= 2\pi \cdot 50 \\ \xi &= 0.7 \\ \nu &= 220 \times 10^{-6}\ g^2/\text{Hz} \end{aligned}\right\} \text{FOR LINEAR ACCELEROMETERS}$$

$$\left.\begin{aligned} \omega_o &= 2\pi \cdot 40 \\ \xi &= 0.6 \\ \nu &= 60.32 \times 10^{-3}\ (\text{rad/sec}^2)^2/\text{Hz} \end{aligned}\right\} \text{FOR ANGULAR ACCELEROMETERS}$$

$$\left.\begin{aligned} \omega_o &= 2\pi \cdot 80 \\ \xi &= 0.5 \\ \nu &= 251.3 \times 10^{-6}\ (^\circ/\text{sec})^2/\text{Hz} \end{aligned}\right\} \text{FOR RATE GYROS}$$

The control computer system has four major components: the MDIS computer, the EDS computer, the 1553 bus system, and the remote units.

The MDIS computer controls the overall operation of the system. It governs the modes of operation, the communication to and from the Shuttle, and the collection and dissemination of control data and commands.

The EDS computer performs the computations necessary to execute a user's control algorithm. It receives data directly from the remote units, processes it, and sends its commands to the remote units, all as coordinated by the MDIS.

The 1553 data bus serves as the communication link among the other parts of the system.

The remote units are located at the various bays along the length of the mast. Each unit governs the operation of the instrumentation at its own particular bay. On command, it collects data from each of the instruments, formats it, and sends it on the 1553 bus. In similar fashion it receives data from the bus, decodes it, and distributes it to the actuators.

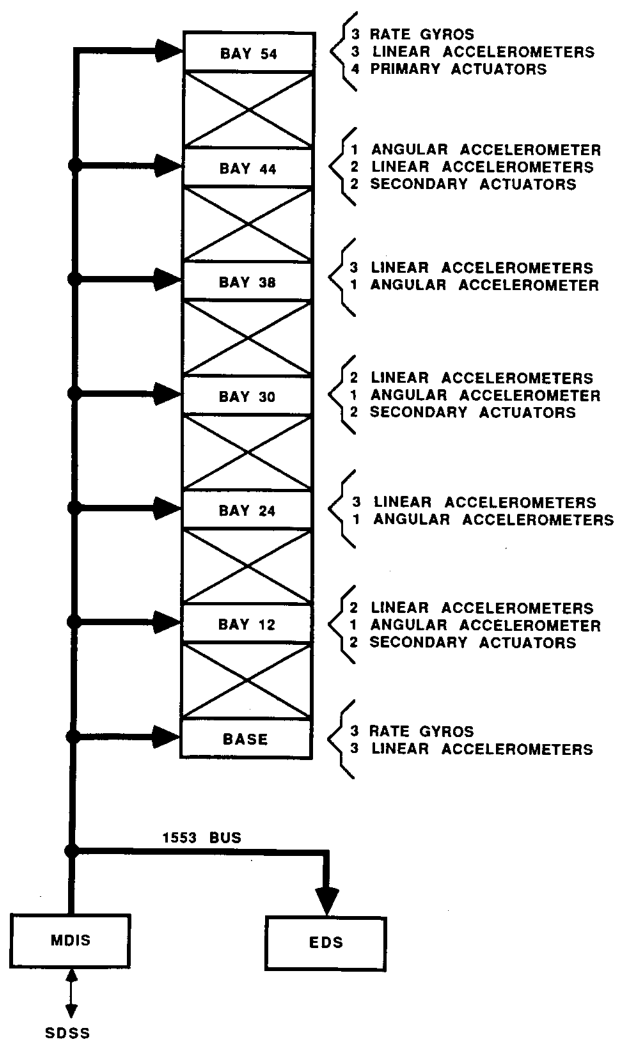

1553 BUS TRANSFER AND PROCESS INTERVAL ALLOCATIONS

The operation of the computer system during one cycle is shown below. First, data is transmitted from the EDS computer to the remote units, which then distribute them to the actuators. At the same time, the remote units collect the sensor data for the next cycle. This data is then sent back down to the EDS computer for processing. The user's algorithm is executed, and a new cycle is begun.

The computer system keeps the jitter under 30 microseconds for one cycle. This ensures clean, distortion free operation of the control algorithms.

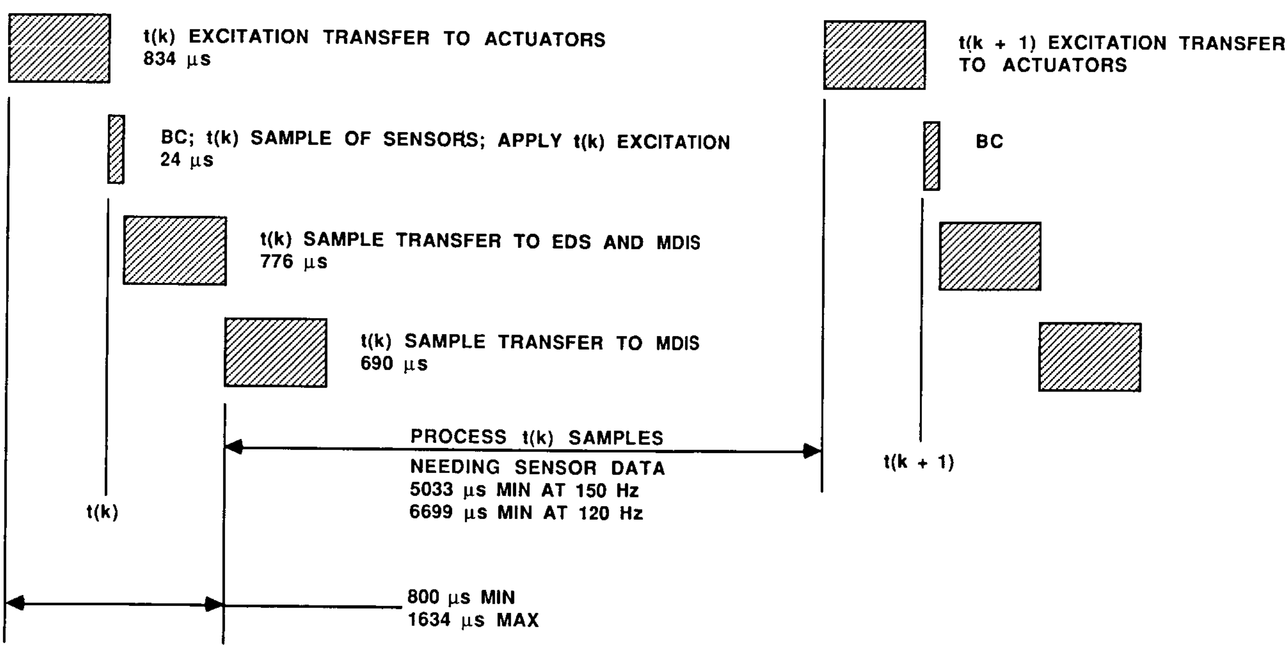

BASELINE DAMPING ALGORITHM

The MAST Flight System includes a baseline damping control algorithm. This algorithm is used as a backup in the case of user algorithm failure or between testing periods to bring the system to a quiescent state.

Harris has developed a baseline control system that is designed to damp the first 10 modes of the mast safely and reliably. It achieves the goal of 5% damping of these modes while operating within the constraints of the hardware. The decentralized approach uses the concepts of positive real design to assure that the stated goals will be achieved in spite of unexpected mission variations.

The damping system operates by first canceling the two poles of the LDCM, then introducing two additional poles: one pole cancels a zero of the LDCM transfer function, the other determines the frequency at which the damping operation of the loop begins. The parameters of the compensators at the various stations are tailored to the modes which the stations affect. Of particular interest is the trade-off between the damping achieved and the actuation level required. The parameters are adjusted to balance these two factors.

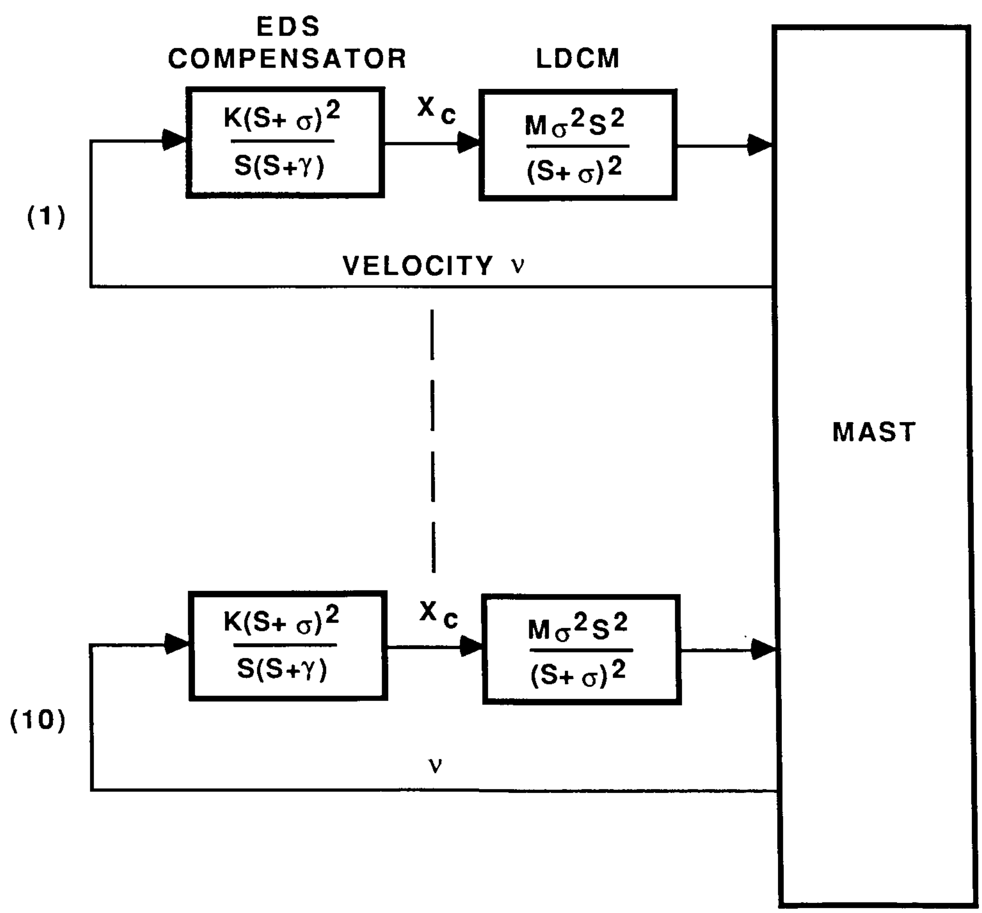

The baseline algorithm was applied to the fully extended mast having the modal characteristics as shown. The modes apply to a mast connected to a simple STS model.

The units of interest are MKS. The modal coefficients are amplitude normalized such that the maximum coefficient of any degree of freedom in the model is unity. Mass normalized modes can be obtained by dividing the given coefficients by the square root of the generalized mass shown for the corresponding mode.

MAST Flight System Modal Data (Includes Orbiter)
Beam Length 54 Bays, Maximum PMD Inertia, LDCMs Locked

BAY	COMP.	1 1st x-z	2 1st y-z	3 2nd y-z	4 2nd x-z	5 1st Torsion	6 3rd y-z	7 3rd x-z	8 2nd Torsion	9 4th y-z	10 4th x-z
12	X	.0344	.0001	.0044	.4196	.0083	.0059	.9047	.0014	-.0004	.9968
	Y	-.0007	-.1431	.3939	-.0027	-.0152	.8858	-.0052	-.0106	.9892	-.0006
	θz	.0002	.0000	.0197	-.0124	.2686	.0190	-.0070	.7243	.0155	-.0053
24	X	.2189	-.0008	.0086	.9158	.0191	.0032	.6197	.0024	-.0006	-.5821
	Y	-.0006	.0125	.8948	-.0063	-.0355	.6240	-.0044	-.0126	-.5645	-.0006
	θz	-.0003	.0000	.0375	-.0231	.5229	.0203	-.0064	1.0000	-.0091	.0043
30	X	.3486	-.0014	.0090	.9830	.0207	-.0006	-.0095	.0008	.0000	-.8769
	Y	-.0004	.1600	.9682	-.0075	-.0387	.0004	-.0006	-.0072	-.8642	.0000
	θz	-.0003	.0000	.0454	-.0280	.6401	.0153	-.0046	.9090	-.0170	.0074
38	X	.5481	-.0024	.0070	.7800	.0166	-.0045	-.7236	-.0019	.0003	.2165
	Y	-.0001	.4072	.7745	-.0061	-.0316	-.7157	.0043	.0023	.2060	.0003
	θz	-.0004	.0000	.0545	-.0338	.7810	.0617	-.0015	.5473	-.0120	.0058
44	X	.7111	-.0033	.0037	.4335	.0094	-.0044	-.7747	-.0025	.0002	.8883
	Y	.0002	.6133	.4337	-.0035	-.0187	-.7702	.0049	.0050	.8701	.0002
	θz	-.0004	.0000	.0604	-.0376	.8743	.0003	.0008	.1687	-.0045	.0025
54	X	.9997	-.0047	-.0038	-.3883	.0080	.0016	.2212	.0006	-.0003	-.1605
	Y	.0008	1.0000	-.3807	.0031	.0120	.2187	-.0015	-.0011	-.1572	.0002
	θz	-.0004	-.0001	.0680	-.0426	1.0000	-.0063	.0036	-.4967	.0004	-.0023
f*		0.1813	0.2387	1.2276	1.2773	1.3004	3.5079	3.6584	4.3637	6.0100	6.2370
$\bar{M}$**		470.46	802.76	260.71	264.12	130.76	223.43	227.79	82.97	266.61	273.68

* Natural Frequency, Hz
** Generalized Mass, kg or kg-m^2 as appropriate

54 BAY POLE SHIFTS FOR BASELINE

The pole locations shown indicate that the goal of 5% damping has been achieved. The open-loop damping reflects an assumption of 0.2% damping for the first bending modes, 0.3% damping for the second bending modes, and 0.5% damping for all higher modes.

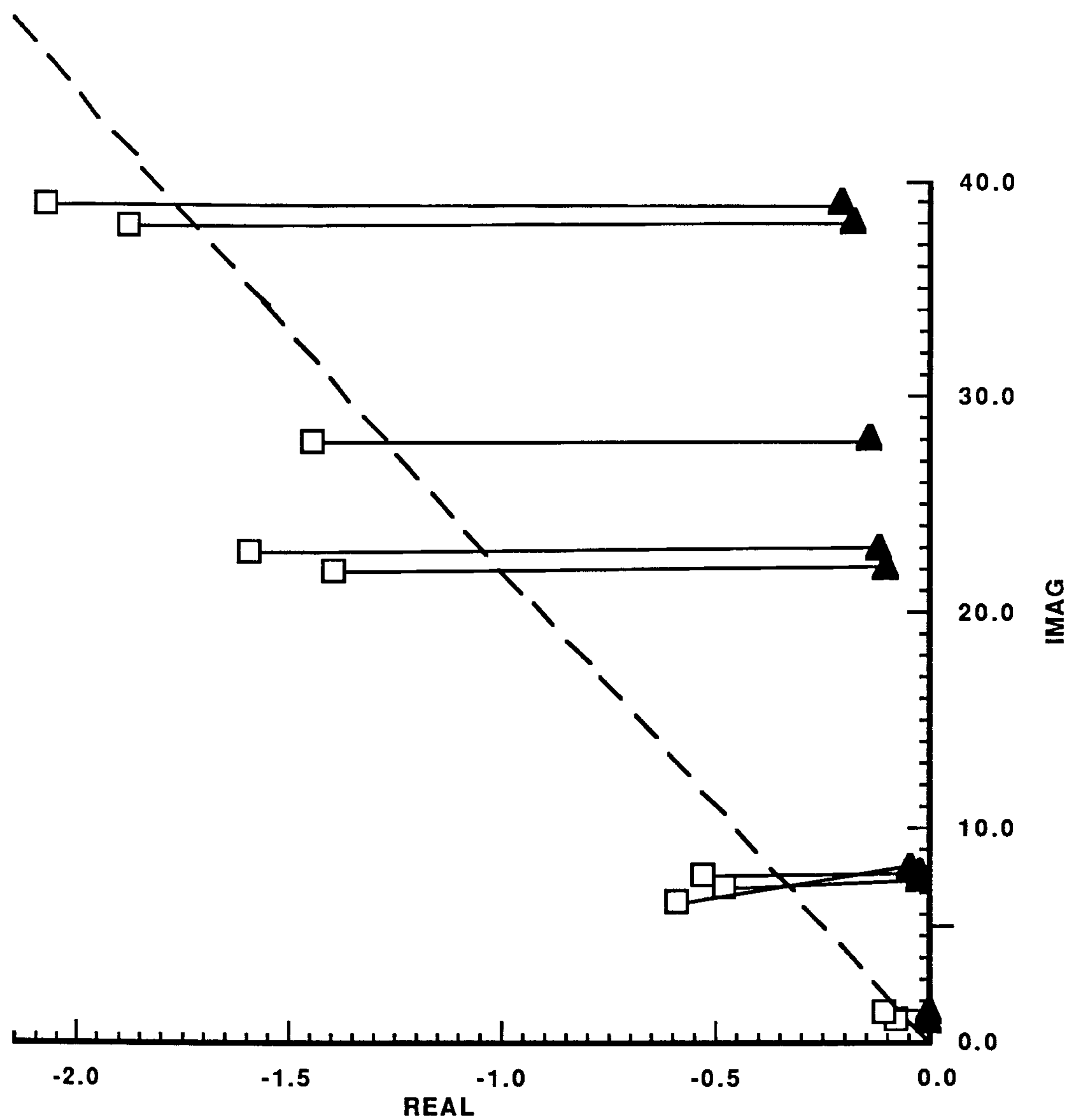

54 BAY POLE SHIFTS FOR BASELINE

DISTURBANCE PSD

Random excitation was applied at bay 44 in the x and y directions to both the open- and closed-loop systems. The other stations were used for control in the closed loop. The disturbance was as shown in the diagram. Independent disturbances were applied in the x and y directions.

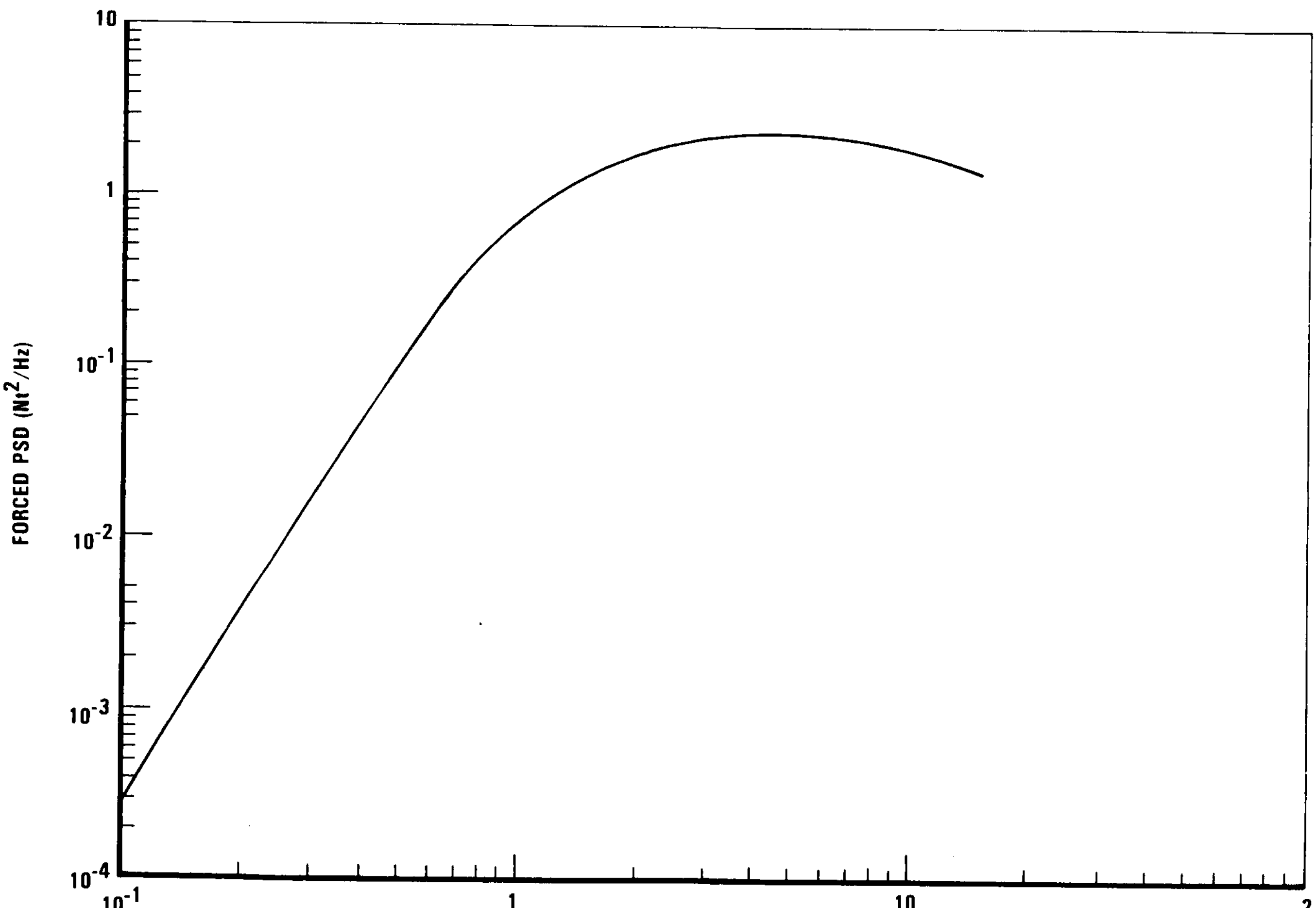

DISTURBANCE PSD (EACH AXIS)

TIP X ACCELERATIONS

The acceleration power spectral densities (PSDs) for the mast tip in the x direction are shown here for the open- and closed-loop cases. It is easy to see the marked smoothing achieved by the control system. In both cases, sufficient signal is detected to be measured by the available sensors.

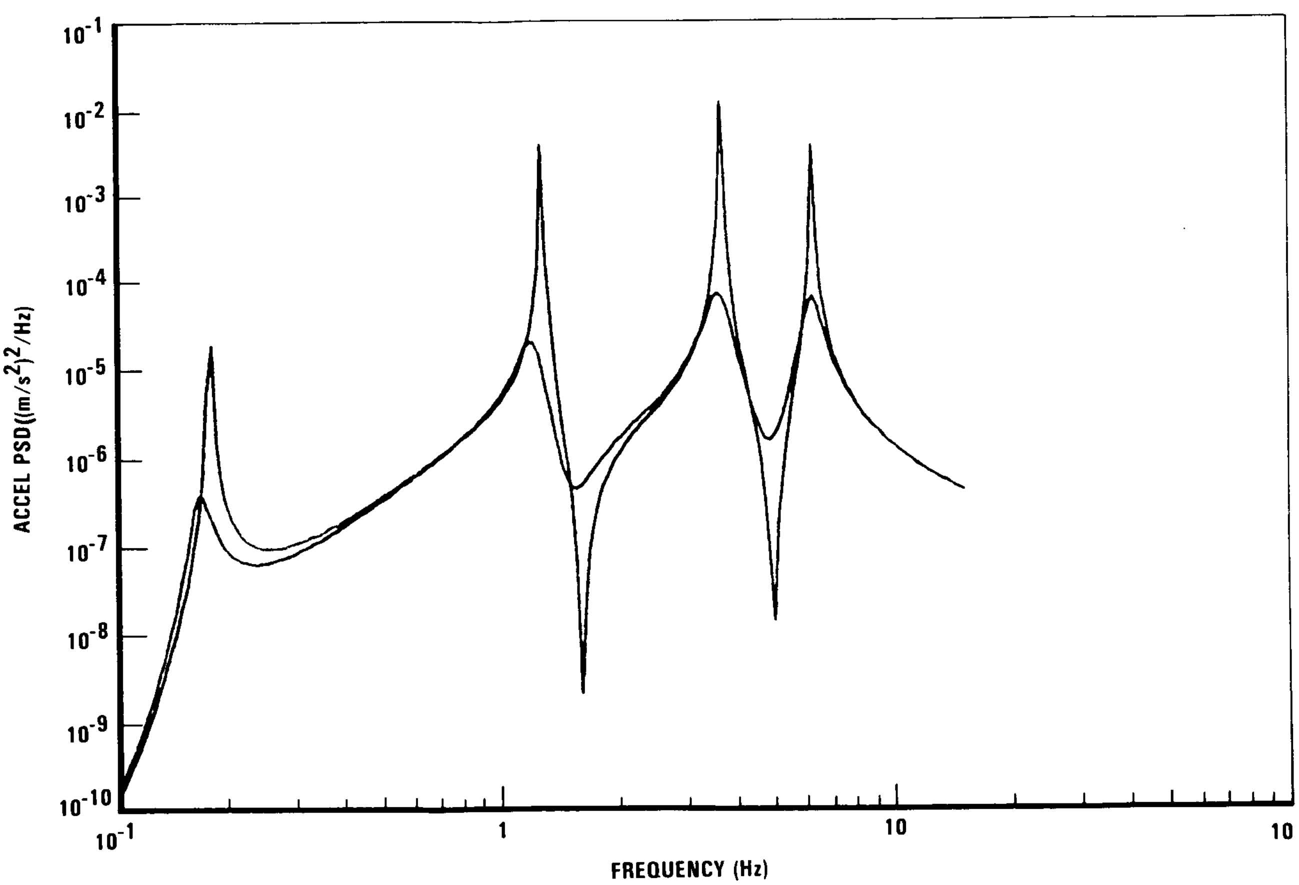

TIP X ACCELERATIONS

TIP Y ACCELERATIONS

Similar results are shown here for the y direction at the mast tip. Once again, marked smoothing of the PSD curve is indicative of the improvement in damping achieved by the control system.

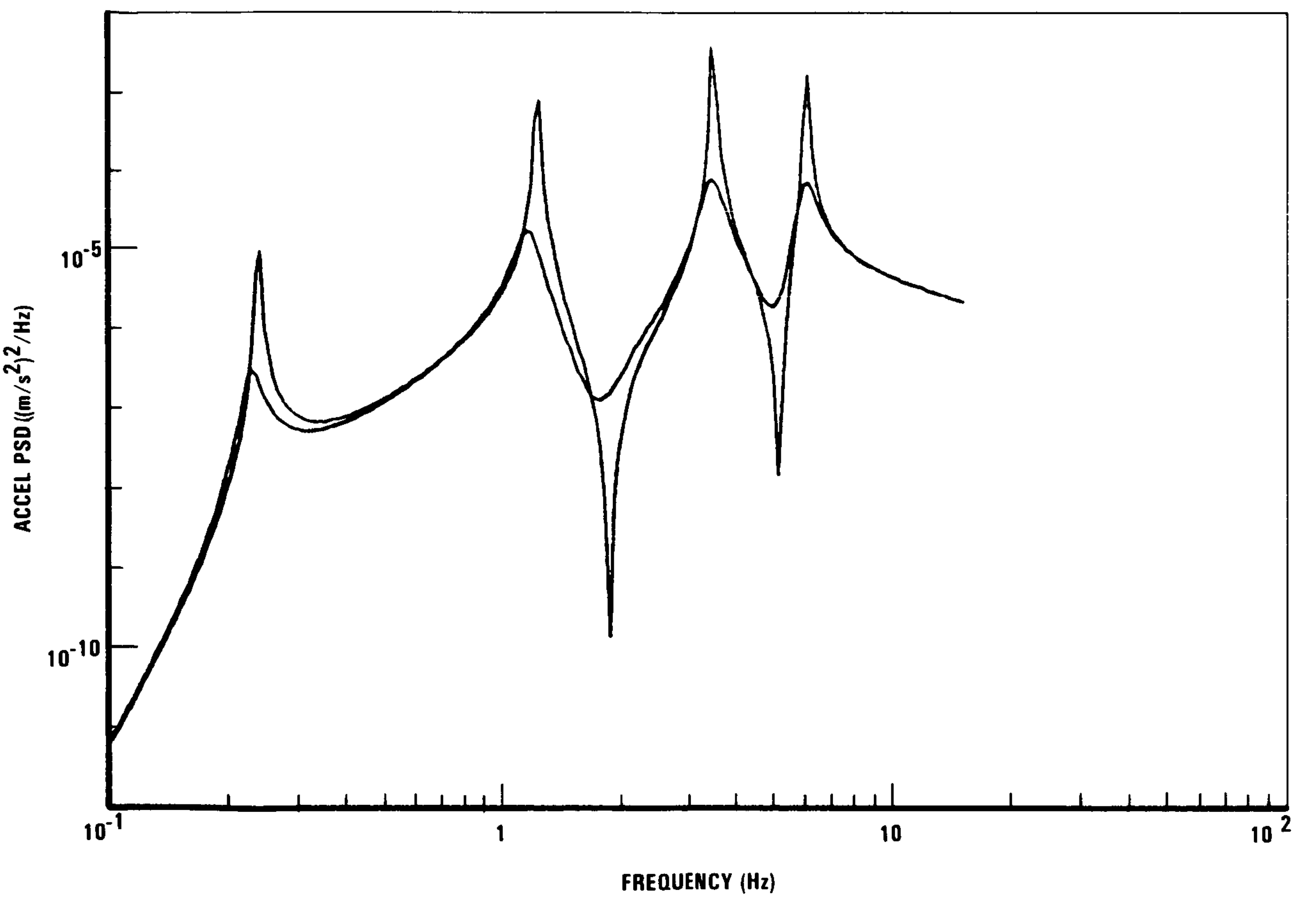

TIP Y ACCELERATIONS

TIP Z ROTATIONAL ACCELERATIONS

The torsion results shown in this diagram, while smoothed, are not as clear-cut as the bending results. This is due chiefly to the lack of direct torsion excitation by the disturbance. In this case, excitation is due to the coupling of the bending and torsion modes and to residual spillover of the control system at the mast tip.

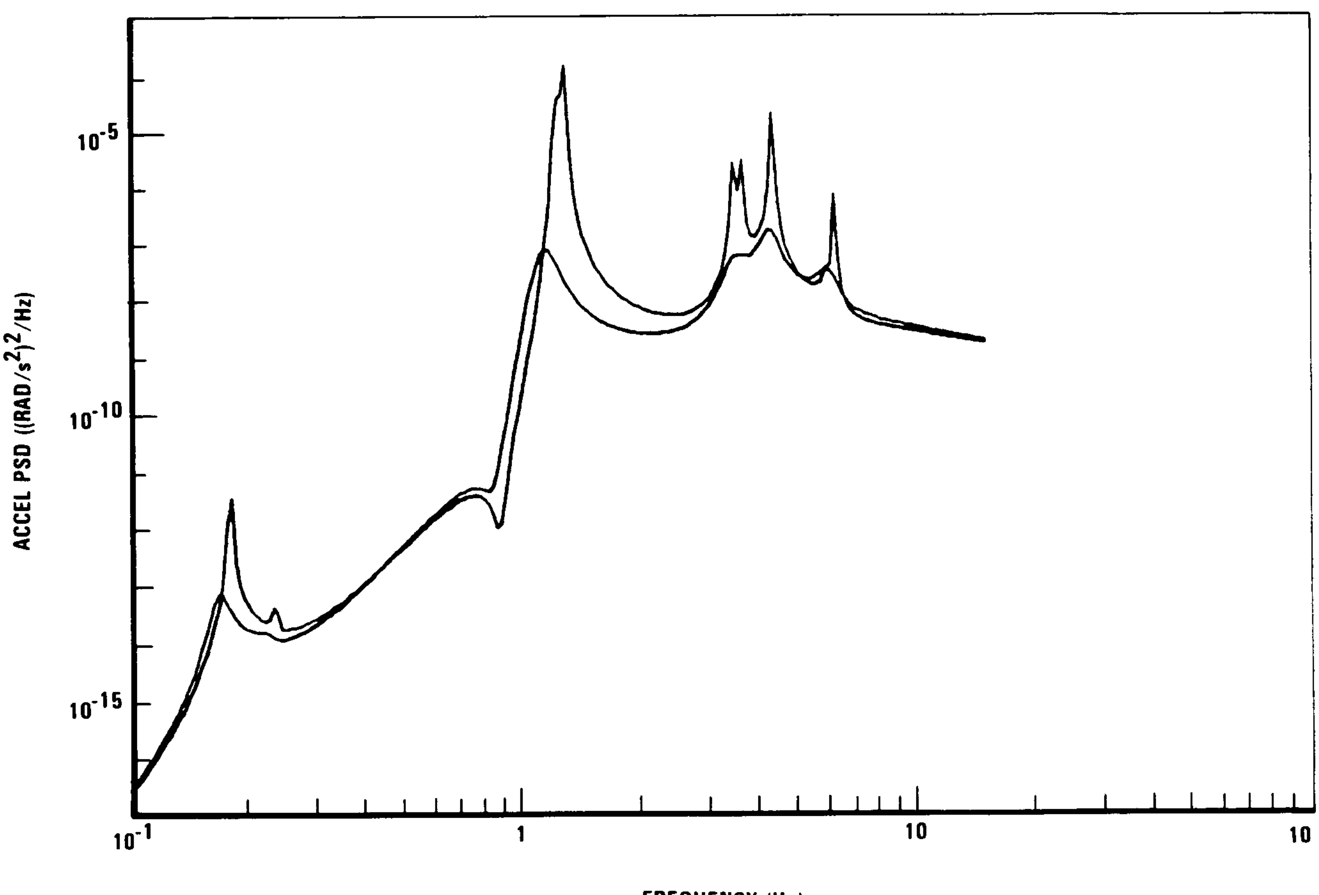

TIP Z ROTATIONAL ACCEL